Case Studies in Thermal Engineering 44 (2023) 102831

Contents lists available at ScienceDirect

Case Studies in Thermal Engineering

journal homepage: www.elsevier.com/locate/csite

Thermal analysis in an electrically conducting fluid with multiple slips and radiation along a plate: A case study of Stokes' second problem

Farwa Asmat [a], W.A. Khan [b], Usman [c,*], MD Shamshuddin [d], S.O. Salawu [e], Mohamed Bouye [f]

[a] School of Mathematical Sciences, Peking University, Beijing, 100871, PR China
[b] Department of Mechanical Engineering, College of Engineering, Prince Mohammad Bin Fahd University, Al Khobar, 31952, Kingdom of Saudi Arabia
[c] Department of Computer Science, National University of Sciences and Technology, Balochistan Campus (NBC), Quetta, 87300, Pakistan
[d] Department of Mathematics, School of Sciences, SR University, Warangal, 506371, Telangana, India
[e] Department of Mathematics, Bowen University. Iwo, Nigeria
[f] Department of Mathematics, College of Science, King Khalid University, PO Box 9004, Abha, 61413, Saudi Arabia

ARTICLE INFO

Keywords:
Stokes second problem
Newtonian fluid
Multiple slips
Thermal radiation
Viscous dissipation
Flat plate
Analytical solution

ABSTRACT

Stoke's problems significantly impact several domains, including industrial manufacturing, geophysical flows, chemical engineering, and heat conduction. Stoke's second problem deals with the movement of a semi-infinite viscous incompressible fluid caused by an oscillating flat plate. Thus, this work examines Stoke's second problem for an unsteady hydromagnetic surface-driven flow along an infinite flat plate in the presence of thermal radiation and heat dissipation. The governing momentum and energy equations form an emerging nonlinear system of partial differential equations through dimensionless proxies. MAPLE 2022 is employed to solve the resulting system of nonlinear partial differential equations that control the flow both analytically and numerically in specific situations. The analytical solutions are displayed graphically, along with variations of skin friction and Nusselt number at the plate. It has been observed that momentum and thermal slips significantly diminished the flow characteristics to cause damping flow rate and temperature distributions. Rising the values of Magnetic and velocity slip parameters, an oscillatory motion is observed in skin friction. This is due to the periodic and wavy nature of the boundary wall. Furthermore, a rise in the Prandtl number and radiation value correspondingly boosted the wall heat gradient profiles. Finally, this study will assist industry and engineering in understanding the sensitivity of their working fluids to parameter variations and for the exact prediction of their base fluids.

1. Introduction

The investigation of thermal propagation and laminar viscous flowing liquid along a slippery moving plate is gaining an increasing research interest in the area of dynamics of fluid due to rising industrial and engineering demands. Pramanik [1] investigated the

* Corresponding author.
E-mail addresses: farwaasmat@pku.edu.cn (F. Asmat), wkhan1956@gmail.com (W.A. Khan), usman.malik.ms@gmail.com (Usman), shammaths@gmail.com, md.shsmshuddin@sru.edu.in (M. Shamshuddin), kunlesalawu2@gmail.com (S.O. Salawu), medeni.doc@gmail.com (M. Bouye).

https://doi.org/10.1016/j.csite.2023.102831
Received 20 October 2022; Received in revised form 29 January 2023; Accepted 18 February 2023
Available online 20 February 2023

effects of suction/blowing and thermal radiation on the flow field and heat transfer in the boundary layer of a Casson fluid over an exponentially stretching sheet. It appears that the study found that these factors can significantly influence the flow field and heat transfer in the presence of suction or injection at the wall. Gupta and Gupta [2] investigated heat and mass transfer using suction or blowing on a stretching sheet. The assertion made by Ref. [2] for a stretchable continuous boundary layer flow with various geometries and thermofluidic conditions, as obtained in Refs. [3–7], was supported by several researchers. Such a flow is helpful in polymer extraction, optical modulation, copper wire production, fiber filters, and others. During material production and cooling or heating of thermal devices, the slip kinematics strongly impact the final product quality, Madhu et al. [8]. Fatunmbi and Adeosun [9] discussed the flow of nanofluid Eyring-Powell along a Riga plate and nonlinear boundary stretching layer. The slip velocity was reported to have enhanced nanofluid Eyring-Powell flow rate resulting from a reduced molecular bond. Waqas et al. [10] examined the heat transfer of hybrid magneto-nanofluid in a nonlinear stretching cylinder. It was discovered that heat distribution is boosted with rising slip parameters. Qureshi [11] studied the flow of hybrid nano-liquid Prandtl-Eyring past an irregular horizontal stretching velocity plate. As seen, the flow velocity and heat transfer are greatly influenced by the nonlinear horizontal moving plate velocity. Few more momentous reports on the nonlinear plate slip can be taken from Refs. [12–15].

The applications of stretching nonlinear boundary layers in thermal science, industry, and technology can be improved when an induced electromagnetic fluid is considered. As reported by Refs. [16,17], the fluid flow rate can be dragged, and the lubricant viscosity of a fluid can be boosted in the present magnetic field. Hence, the study of hydromagnetic flow is encouraged due to its many applications in nuclear reactors, MHD power generators, agricultural engineering, petroleum, and others. As such, Bhatti et al. [18] investigated non-Newtonian nano flow of entropy-generated fluid through a porous slippery sheet with a magnetic field. The study noticed that the magnetic field resists flow motion but boosts temperature distribution. Khan et al. [19] presented hybrid material fluid flow with varying magnetic fields in an elongated sheet. It was seen that near the boundary layer, the body force accelerated due to the Lorentz force inspired by a magnetic field. More findings on hydromagnetic flow in a stretching slip velocity can be obtained from Refs. [20–24]. However, in a heat transfer system involving high temperature, radiation is an essential thermodynamic physical quantity, for instance, in glass sheets or metal cooling. Due to its usage, Unyong [25] discussed, in a thermofluidic system, the effect of radiation and entropy generation in an inclined magnetic field. The results depicted that heat radiative raised the heat transfer profile. Sharma et al. [26] examined heat radiative and dissipation of hydromagnetic flow with variable viscosity through a stretching boundary layer. The shear stress rate was reported to have been augmented with rising thermal radiation. More also, Mabood and Das [27] adopted the Rosseland approximation model for the thermal radiation of hydromagnetic flow past a second-order stretchy slip surface with melting heat distribution. The flow characteristics were presented to have been significantly influenced by the radiation and second-order slip terms. Meanwhile, Stoke's second problem was not considered in all the aforementioned studies.

Stoke's second problem is a periodic continuous flow, which is emblematic of Newtonian fluid flow dynamics. Thermal fluid transfer served as a working fluid in many industries. By adopting a numerical scheme, Chen and Chen [28] considered second grade for a generalized Stoke problem. Khan et al. [29] studied nanofluid heat transfer for Stoke's second problem: A thermal engineering application. The study displayed rising heat distribution in the presence of the fluid material. Bedrikova and Latyshev [30] investigated the second Stoke's flow model past an oscillatory surface for gas variable amplitude. An analytical solution was presented to show the impact of thermofluidic terms. Ishfaq et al. [31] carried out a comprehensive analysis of fluid material Stoke's second-order model. The thermophoretic was announced to have increased the chemical reaction. Duan and Qiu [32] presented a constitutive model for a viscoelastic Stoke's second fluid problem. The viscoelastic material term dragged the flow velocity distribution. Hor et al. [33] examined asymmetry heat boundary layer viscous dissipation of Stoke's second model flow in a microchannel.

Of the many considered studies, no model and discussion on the hydromagnetic thermal radiation in multiple slips have been examined despite its usefulness in the area of technology and science. As such, this study focuses on Stoke's second problem of multiple nonlinear slips with thermal radiation, heat dissipation, and uniform magnetic field. The significance of thermodynamic fluid properties in industry and thermal science has motivated this study. Hence, the developed model is solved analytically, and the outcomes are offered in graphs to demonstrate the strength of the fluid terms and response of the flow characteristics.

2. Model formulation

Consider a laminar flow of an incompressible Newtonian fluid along an infinite flat plate, as shown in Fig. 1. The x-axis is aligned

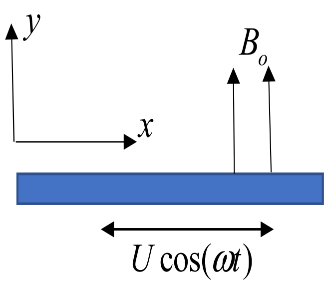

Fig. 1. Schematic of Stokes' second problem.

with the plate. At the same time, the y-axis is perpendicular to the plate. The pressure gradient and body forces are neglected. A uniform magnetic field B_0 is applied normally to the plate. It is assumed that the induced magnetic field is negligible. The thermo-physical properties of the fluid are assumed to be constant. At the time $t = 0+$, the plate starts to flow and move in its plane with velocity $U\cos(\omega t)$. As $y \to \infty$, the velocity declines to zero. The plate surface is exposed to first-order velocity and thermal slip. The ambient temperature and the plate temperature are assumed to be T_w. The effects of viscous dissipation and radiation effects are introduced in the energy equation.

The momentum and energy equations for Stoke's second problem can be written as

$$\frac{\partial u(y,t)}{\partial t} = \nu_f \frac{\partial^2 u(y,t)}{\partial y^2} - \frac{\sigma B_o^2}{\rho_f} u(y,t) \tag{1}$$

$$\frac{\partial T(y,t)}{\partial t} = \alpha_f \frac{\partial^2 T(y,t)}{\partial y^2} - \left(\frac{1}{\rho c_p}\right)\frac{\partial q_r}{\partial y} + \left(\frac{\mu}{\rho c_p}\right)\Phi \tag{2}$$

The viscous dissipation function Φ and the radiative heat flux q_r can be defined as

$$\Phi = \left(\frac{\partial u}{\partial y}\right)^2 \text{ and } q_r = -\frac{4\sigma_1}{3k_1}\frac{\partial T^4}{\partial y} \tag{3}$$

The term T^4 can be expanded using the Taylor series and written as $T^4 \cong 4T_\infty^3 T$(neglecting higher order terms). Therefore, the energy equation is given by

$$\frac{\partial T(y,t)}{\partial t} = \left[\alpha_f + \frac{16\sigma_1 T_\infty^3}{3(\rho c_p)_f k_1}\right]\frac{\partial^2 T(y,t)}{\partial y^2} + \left(\frac{\mu}{\rho c_p}\right)\left(\frac{\partial u}{\partial y}\right)^2 \tag{4}$$

with the initial and boundary conditions

$$\begin{aligned} u(0,t) &= u_o\cos(\omega t) + L_s\left(\frac{\partial u}{\partial y}\right) t > 0 \\ T(0,t) &= T_w + \mathrm{L_t}\frac{\partial T}{\partial y} t > 0 \\ u(y,0) &= 0; T(y,0) = 0 y > 0 \\ u(y,t) &\to 0; T(y,t) = T_\infty \quad \mathrm{y} \to \infty \end{aligned} \tag{5}$$

where ν_f, α_f, ω, Φ, $(\rho c_p)_f$, σ_1 and k_1 are the kinematic viscosity, thermal diffusivity, frequency of the velocity of the plate, dissipation function, the heat capacitance of the fluid, the Stefan-Boltzmann constant and the mean absorption coefficient, respectively.

Introducing the following dimensionless quantities in Eqns. (1)–(3):

$$U = \frac{u}{u_0}; \tau = \omega t; \eta = y\sqrt{\frac{\omega}{\nu_f}}; \theta = \frac{T - T_\infty}{T_w - T_\infty} \tag{6}$$

We obtain the following dimensionless equations and corresponding boundary conditions:

$$\frac{\partial U}{\partial \tau} = \frac{\partial^2 U}{\partial \eta^2} - MU \tag{7}$$

$$\frac{\partial \theta}{\partial \tau} = \frac{1}{\Pr}(1 + Rd)\frac{\partial^2 \theta}{\partial \eta^2} + Ec\left(\frac{\partial U}{\partial \eta}\right)^2 \tag{8}$$

with initial and boundary conditions

$$\begin{aligned} U(0,\tau) &= \cos(\tau) + \alpha\frac{\partial U}{\partial \eta} \tau > 0 \\ U(\eta,0) &= 0; \theta(\eta,0) = 0 \eta > 0 \\ U(\eta,\tau) &\to 0; \theta(\eta,\tau) \to 0 \eta \to \infty \\ \theta(0,\tau) &= 1 + \beta[\theta'(0,\tau)] \quad \text{for } \tau > 0 \end{aligned} \tag{9}$$

where $M = \frac{\sigma B_o^2}{\rho_f \omega}$ is the magnetic parameter, $R_d = \frac{16\sigma_1 T_\infty^3}{3k_f\ k_1}$, $\Pr = \frac{\nu_f}{\alpha_f}$ and $Ec = \frac{u_o^2}{c_p \Delta T_w}$ are the radiation parameter, Prandtl and Eckert numbers, α is the velocity slip parameter, β is the temperature slip parameter.

3. Solution methodology

The momentum equation can be solved analytically, following [34] and assuming,

$$U(\eta,\tau) = \mathrm{Re}\left[W(\eta).e^{i\tau}\right] \tag{10}$$

where Re designates the real part of the quantity inside the square bracket. Substituting Eq. (10) into Eq. (5), we get the following second-order differential equation:

$$W''(\eta) - i(1 - iM)W(\eta) = 0 \tag{11}$$

Using $\sqrt{\mathrm{i}} = \dfrac{1+i}{\sqrt{2}}$, the general solution of (5) can be written as

$$\mathrm{W}(\eta) = C_1 \exp\left[\frac{1+i}{\sqrt{2}}\sqrt{1-iM}\ \eta\right] + C_2 \exp\left[-\frac{1+i}{\sqrt{2}}\sqrt{1-iM}\ \eta\right] \tag{12}$$

The condition of finite velocity $W(\eta) \rightarrow$ finite when $\eta \rightarrow \infty$ suggests that the constant C_1 should be zero. Thus

$$\mathrm{W}(\eta) = C_2 \exp\left[-\frac{1+i}{\sqrt{2}}\sqrt{1-iM}\ \eta\right] \tag{13}$$

Using Binomial expansion $\sqrt{1-iM} = 1 - \frac{1}{2}iM + \ldots$ neglecting higher order terms, we get

$$\mathrm{W}(\eta) = C_2 \exp\left[-\frac{M+2}{2\sqrt{2}}\ \eta\right]\exp\left[i\frac{M-2}{2\sqrt{2}}\ \eta\right] \tag{14}$$

Therefore, Eq. (10) gives

$$\mathrm{U}(\eta,\tau) = \mathrm{Re}C_2 \exp\left[-\frac{M+2}{2\sqrt{2}}\ \eta\right]\exp\left[i\tau + \frac{M-2}{2\sqrt{2}}\ \eta\right] = C_2 \exp\left[-\frac{M+2}{2\sqrt{2}}\ \eta\right]\cdot\cos\left[\tau + \frac{M-2}{2\sqrt{2}}\ \eta\right] \tag{15}$$

where the constant C_2 can be determined by using the velocity slip condition $U(0,\tau) = \cos(\tau) + \alpha\frac{\partial U}{\partial \eta}$. Differentiating Eq. (15) w.r.t η, we get

$$C_2 = \frac{4\cos\tau}{\alpha\sqrt{2}(2\cos\tau - 2\sin\tau) + 4\cos\tau} \tag{16}$$

Therefore, the dimensionless velocity distribution can be written as

$$\mathrm{U}(\eta,\tau) = \frac{4\cos\tau \exp\left[-\frac{M+2}{2\sqrt{2}}\ \eta\right]\cdot\cos\left[\tau + \frac{M-2}{2\sqrt{2}}\ \eta\right]}{\alpha\sqrt{2}(2\cos\tau - 2\sin\tau) + 4\cos\tau} \tag{17}$$

This shows that the dimensionless velocity oscillates in time with the same frequency as the plate $\eta = 0$. The energy equation is solved numerically using MAPLE 2022. MAPLE is a mathematical software package that is commonly used for symbolic computation, which involves the manipulation of mathematical expressions and equations. It can be used to solve a wide variety of mathematical problems, including those involving differential equations and other complex mathematical expressions.

The solution to the Energy equation using MAPLE involves solving a system of partial differential equations (PDEs) that describe the flow of a viscous fluid. The PDEs can be solved using various techniques, such as finite difference or finite element methods. One way to solve the problem using MAPLE is to use the PDEtools package, which provides a suite of functions for solving PDEs.

pdsolve(sys, ICs union BCs, numeric, time = t, range = 0..N); The spacestep and timestep are kept as 0.001 and 0.01, respectively. This will give the solution for the temperature as a function of y and t in terms of M, Rd, Ec, and Pr. We can use these solutions to calculate other quantities of interest, such as the skin friction and the Nusselt number for different values of governing parameters.

3.1. Quantities of physical interest

The local skin friction factor C_f and the local Nusselt number Nu_x are the quantities of physical interest and can be defined as

$$C_f = \frac{2\tau_w}{\rho_f u_o^2}, \quad Nu_x = \frac{x\, q_w}{k_f(T_w - T_\infty)}, \tag{18}$$

where τ_w, q_w shear stress and the wall heat flux are defined as

$$\tau_w = \mu_f\left(\frac{\partial u}{\partial y}\right)_{y=0}, \quad q_w = -\left(k_f + \frac{16\sigma_1 T_\infty^3}{3k_1}\right)\left(\frac{\partial T}{\partial y}\right)_{y=0}. \tag{19}$$

Using Eqn. (4)

$$\mathrm{Re}_x^{1/2}C_f = 2\frac{\partial U}{\partial \eta}\bigg|_{\eta=0} = \frac{8\cos^2\tau}{\alpha\sqrt{2}[(M+2)\cos\tau + (M-2)\sin\tau] + 4\cos\tau}$$
$$\mathrm{Re}_x^{1/2}Nu_x = -(1+R_d)\theta'(0) \tag{20}$$

4. Graphical interpretation with discussion of results

The study investigates the effects of multiple slips in an unsteady MHD convective flow of a Stokes' second problem across an infinite plate. The two-dimensional partial differential equations are converted into a dimensionless partial differential equations system. The resulting flow equations are solved analytically in exceptional cases and numerically using MAPLE 2022. The impact of parameters influencing fluid flow is thoroughly explored in Figs. 2–11.

Fig. 2(a) and (b) demonstrate the effect of the magnetic parameter on the flow velocity. When a magnetic field is applied to a fluid, it can generate an induced electric field within the fluid, which, in turn, can produce an induced current. This current can interact with the magnetic field to produce a force known as the Lorentz force. In the case of a boundary layer, the Lorentz force can act to reduce the velocity gradient near the solid boundary and can also increase the thickness of the boundary layer. This can lead to a decrease in the friction drag on the solid boundary and a decrease in the heat transfer rate. It is important to notice that the magnetic field must be strong enough to overcome the viscous forces, and it depends on the properties of the fluid and the strength of the magnetic field. The velocity distribution is dampened by varying the magnetic term while holding the other terms constant. The resistance to the flow is caused by the stimulated electromagnetic force, which is created by the magnetic field. The reaction of the flow rate profile to the rising velocity slip term is displayed in Fig. 3(a) and (b). A variation in the term decreases the current carrying second Stoke's fluid along the infinite wavy sheet. As the values are increased, fluid-particle interaction is opposed all over the flow region. In contrast, close to the plate wall, the effect is substantial because of the wall's friction, which causes a decrease in the velocity distribution. The impact of nonlinear thermal slip (β) is investigated in Fig. 4(a) and (b) under the continuous periodic heat transfer $t = 2\pi$ and $t = \pi/2$. As observed, the heat transfer decreases along the infinite plate device due to a decline in the thermal boundary film thickness; this allows thermal diffusion out of the electrically conducting fluid to the surroundings. The effect of the thermal slip parameter on the dimensionless temperature will depend on the specific conditions of the fluid flow and the material properties of the fluid and the solid surface. In general, however, the thermal slip parameter can have an impact on the rate of heat transfer between the solid surface and the fluid, and this can, in turn, affect the dimensionless temperature of the fluid. If the thermal slip parameter is large (indicating that the thermal boundary layer is much thicker than the viscous boundary layer), it can lead to a reduction in the rate of heat transfer between the solid surface and the fluid, and this can result in a lower dimensionless temperature of the fluid. On the other hand, if the thermal slip parameter is small (indicating that the thermal boundary layer is much thinner than the viscous boundary layer), it can lead to an increase in the rate of heat transfer between the solid surface and the fluid, and this can result in a higher dimensionless temperature of the fluid.

Meanwhile, a rise in the Eckert number encourages fluid particle thermal propagation to boost the temperature field, as seen in Fig. 5(a) and (b). The term characterizes the thermal dissipation of heat energy; it depicts the relationship between the boundary enthalpy layer and the flow's kinetic energy. As noticed, the heat dissipation term at different periodic energy transfers raises the temperature distribution. Fig. 6a and b establish the response of the skin friction to respective variations in the magnetic (M) and velocity slip (α) parameters. For both plots, the wall friction decreases significantly near the wall because of the high fluid friction associated with the fluid particle restriction. However, some distance away from the plate surface, a steady rise in the skin friction is noticed due to rising internal heating that breaks the bonding force. The effect of the magnetic parameter on skin friction depends on the specific flow conditions and the properties of the fluid, and the magnetic field. In Fig. 6 (a), the magnetic field leads to a reduction in skin friction, as the magnetic forces acting on the fluid can help to smooth out the flow and reduce viscous resistance. On the other hand, if the magnetic field is too strong, it can lead to an increase in skin friction, as the fluid experiences a greater degree of resistance as it tries to flow past the solid surface. The effect of the velocity slip parameter on skin friction depends on the specific flow conditions and the properties of the fluid and solid surface. In general, as the velocity slip parameter increases, the amount of skin friction at the

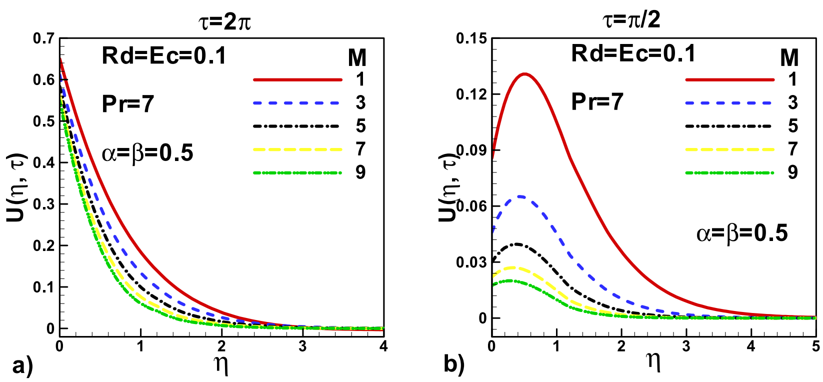

Fig. 2. Effects of magnetic parameter on dimensionless velocity.

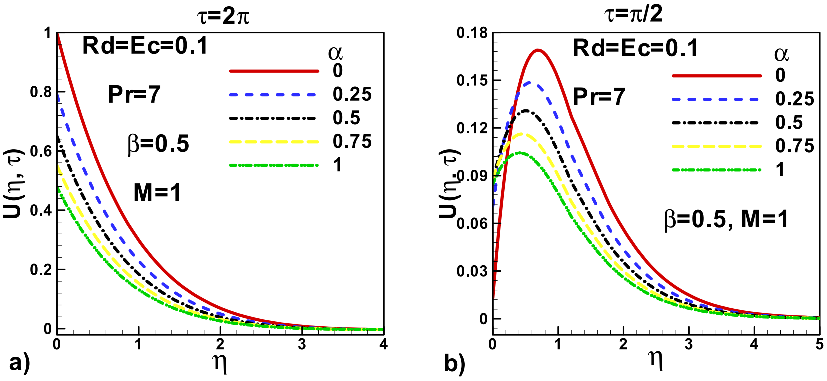

Fig. 3. Effects of velocity slip parameter on dimensionless velocity.

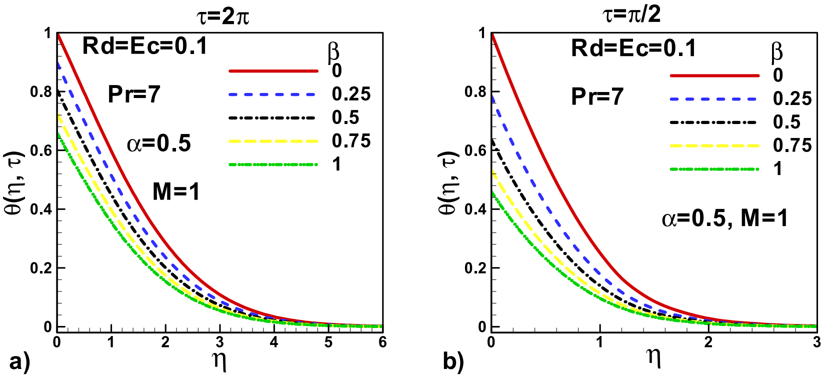

Fig. 4. Effects of thermal slip parameter on dimensionless temperature.

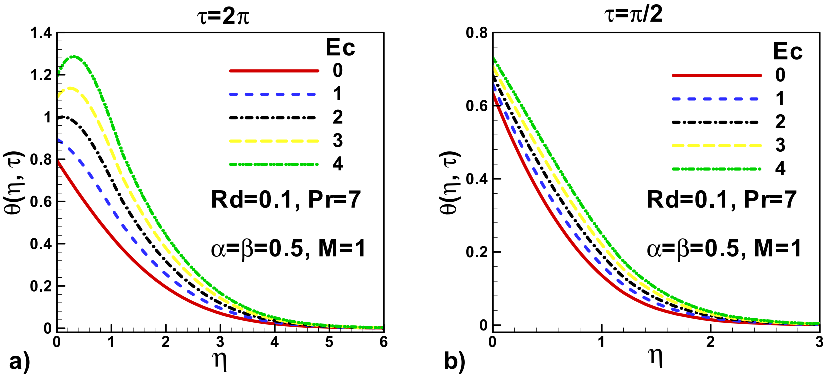

Fig. 5. Effects of viscous dissipation on dimensionless temperature.

boundary also increases. This is because the fluid experiences a greater degree of resistance as it tries to flow past the solid surface, leading to an increase in the frictional forces between the two.

This thereby unrestricted the motion of the fluid particles. Though, far the stream, dampness in the skin friction is noticed as the fluid viscosity dominates the heat generation. As such, the molecular bond is steadily induced, dragging the flow. Fig. 7a and b shows the reaction of the wall heat gradient to rising thermal slip and viscous dissipation terms. The wall heat gradient denotes the Nusselt number, which describes the relationship between thermal convection and heat conduction ratio across the boundary layer. The effect of the thermal slip parameter on the dimensionless heat transfer rate depends on the specific flow conditions and the properties of the fluid and solid surface. In the neighbourhood of the surface, the dimensionless heat transfer rate reaches a maximum value and then decreases with increasing time. When the thermal slip parameter increases, the dimensionless heat transfer rate decreases. This is because the temperature gradient at the surface becomes smaller, leading to a lower rate of heat transfer between the fluid and the

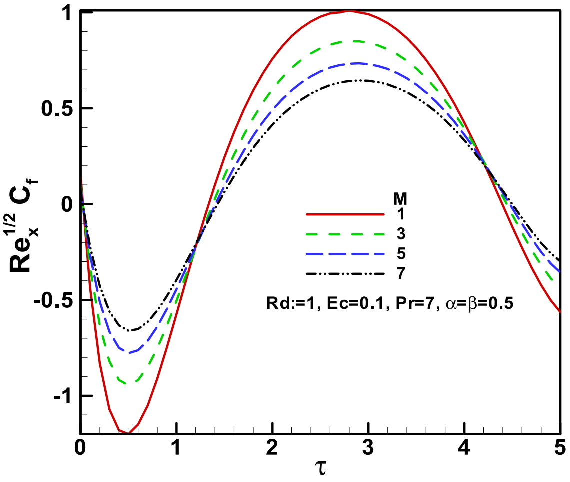

Fig. 6a. Effects of magnetic parameter on skin friction.

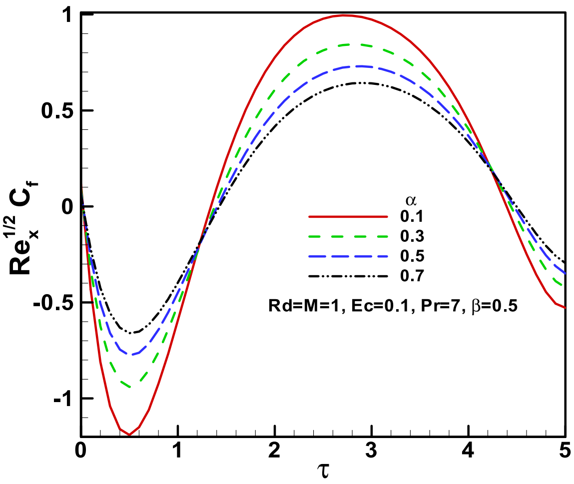

Fig. 6b. Effects of velocity slip parameter on skin friction.

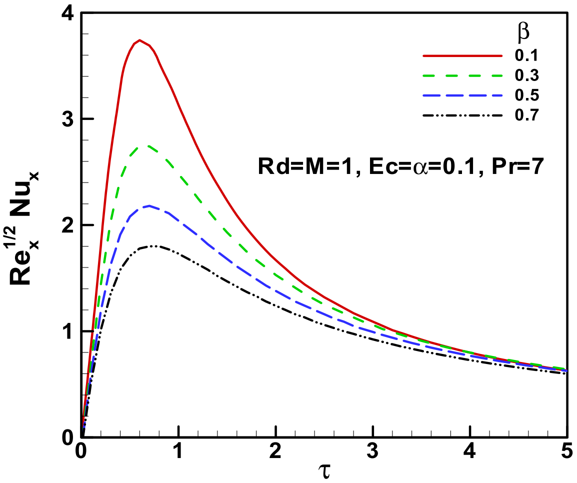

Fig. 7a. Effects of thermal slip parameter on the dimensionless heat transfer rate.

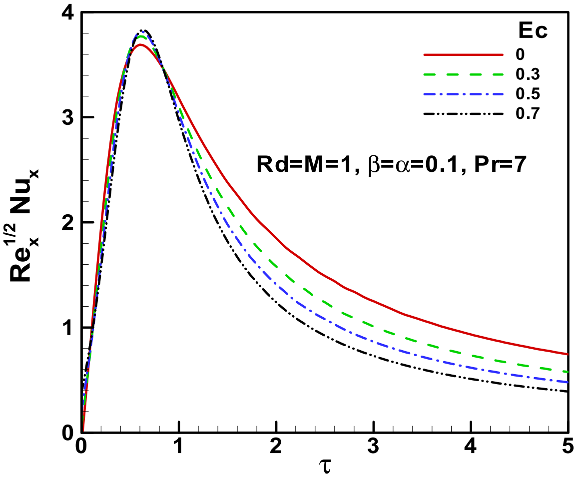

Fig. 7b. Effects of viscous dissipation on the dimensionless heat transfer rate.

solid.

In Fig. 8a and b, the Nusselt number increases as the Prandtl and radiation numbers are raised separately. The fluid flow thermal conduction dominates the wall heat transfer to boost the heat gradient at the wall and the flow regime. The thermal boundary film viscidness is raised to obstruct heat diffusion, propelling the Nusselt number for the rising values of the dynamical fluid parameters.

5. Conclusion

In the study, Stokes' Second problem of an unsteady hydromagnetic surface-driven flow along an infinite wavy sheet in the company of thermal dissipation, radiation, and uniform magnetic field has been executed. Furthermore, the boundary conditions are subjected to nonlinear multiple slip conditions. The objectives are achieved by determining the flow rate, thermal field, wall friction, and Nusselt number profiles for parameter sensitivities. The proposed mathematical model is solved to find the best exploratory solution available. The impacts of variables are pictorially depicted and explained in depth. Based on the results, it can be concluded that:

- Velocity and thermal slips momentously reduced the flow characteristics to cause damping flow rate and temperature distributions.
- The monotonically rise in the $U(\eta,\tau)$ and $\theta(\eta,\tau)$ with increasing η leads to a respective decrease and rise in the thermal fluid flow dimension for variation in M and Ec.
- An oscillatory motion in the skin friction is obtained for rising values of M and α due to the periodic and wavy boundary wall.
- The Prandtl number and radiation value correspondingly increased the wall heat gradient profiles.

Thus, an extension to Arrhenius's kinetics fluid flow in a cylinder and channel is encouraged to improve the application of the second-order Stoke's problem.

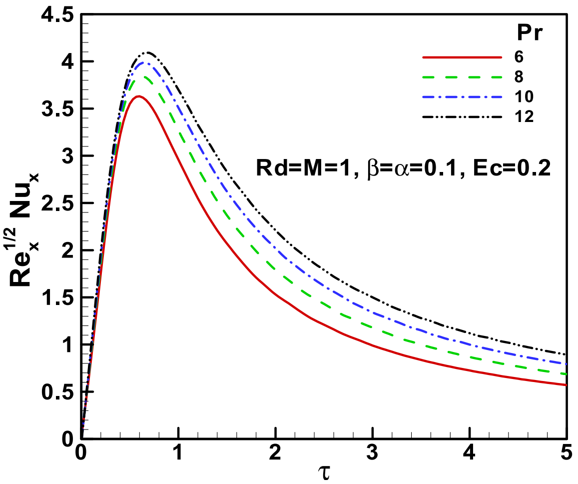

Fig. 8a. Effects of Prandtl number on the dimensionless heat transfer rate.

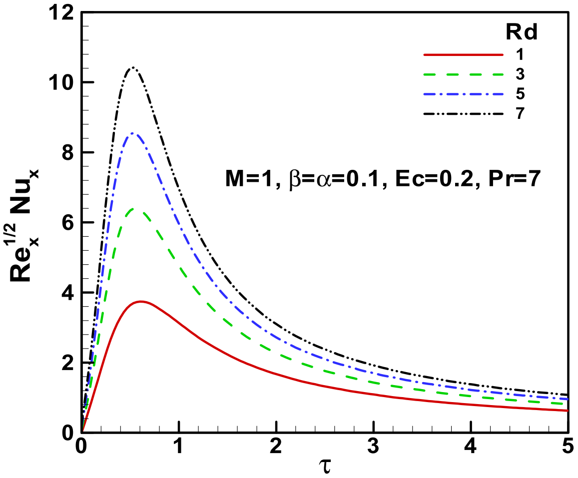

Fig. 8b. Effects of radiation parameter on the dimensionless heat transfer rate.

Author statement

Farwa Asmat: Conceptualization, Software, Validation, ***W.A. Khan***: Software, Analysis. Writing an original Draft. ***Usman:*** Visualization, Data Curation, and Investigation. ***MD. Shamshuddin***: Methodology, Software, Validation. ***S.O. Salawu***: Writing, Reviewing, and Editing. ***Mohamed Bouye***: Supervision, Analysis, Validation.

Declaration of competing interest

The authors declare that they have no known competing financial interests or personal relationships that could have appeared to influence the work reported in this paper.

Data availability

Data will be made available on request.

Acknowledgment

The authors extend their appreciation to the Deanship of Scientific Research at King Khalid University, Abha, Saudi Arabia for funding this work through Large Groups Project under grant number RGP.2/217/43.

References

[1] S. Pramanik, Casson fluid flow and heat transfer past an exponentially porous stretching surface in the presence of thermal radiation, Ain Shams Eng. J. 5 (2014) 205–212.
[2] P.S. Gupta, A.S. Gupta, Heat and mass transfer on a stretching sheet with suction or blowing, Can. J. Chem. Eng. 55 (1997) 744–756.
[3] E. Magyari, B. Keller, Heat and mass transfer in the boundary layers on an exponentially stretching continuous surface, J. Phys. D Appl. Phys. 32 (1999) 577–585.
[4] A.M. Okedoye, S.O. Salawu, Effect of nonlinear radiative heat and mass transfer on MHD flow over a stretching surface with variable conductivity and viscosity, J. Serbian Soc. Comput. Mech. 13 (2) (2019) 87–104.
[5] E. Sanjayanand, S.K. Khan, On heat and mass transfer in a viscoelastic boundary layer flow over an exponentially stretching sheet, Int. J. Therm. Sci. 45 (2006) 819–828.
[6] S.K. Khan, Boundary layer viscoelastic fluid flow over an exponentially stretching sheet, Int. J. Appl. Mech. Eng. 11 (2006) 321–335.
[7] M.D. Shamshuddin, G.R. Rajput, W. Jamshed, F. Shahzad, S.O. Salawu, A. Aissa, V.S. Patil, MHD bioconvection microorganism nanofluid driven by a stretchable plate through porous media with an induced heat source, Waves in Random and Complex Media, 2022, https://doi.org/10.1080/17455030.2022.2126024.
[8] M. Madhu, N. Kishan, A.J. Chamkha, Unsteady flow of a Maxwell nanofluid over a stretching surface in the presence of magnetohydrodynamic and thermal radiation effects, Propuls. Power Res. 6 (1) (2017) 31–40.
[9] E.O. Fatunmbi, A.T. Adeosun, Nonlinear radiative Eyring-Powell nanofluid flow along a vertical Riga plate with exponential varying viscosity and chemical reaction, Int. Commun. Heat Mass Tran. 119 (2020), 104913.
[10] H. Waqas, S.M.R.S. Naqvi, M.S. Alqarni, T. Muhammad, Thermal transport in magnetized flow of hybrid nanofluids over a vertical stretching cylinder, Case Stud. Therm. Eng. 27 (2021), 101219.
[11] M.A. Qureshi, A case study of MHD-driven Prandtl-Eyring hybrid nanofluid flow over a stretching sheet with thermal jump conditions, Case Stud. Therm. Eng. 28 (2021), 101581.
[12] M.D. Shamshuddin, C. Balarama Krishna, Heat absorption and Joule heating effects on transient free convective reactive micropolar fluid flow past a vertical porous plate, Fluid Dynam. Mater. Process. 15 (3) (2019) 207–231.
[13] A.R. Hassan, S.O. Salawu, A.B. Disu, O.R. Aderele, Thermodynamic analysis of a tangent hyperbolic hydromagnetic heat generating fluid in quadratic Boussinesq approximation, J. Comput. Math. Data Sci. 4 (2022), 100058.
[14] W. Jamshed, S.U. Devi, S.M. Goodarzi, M. Prakash, K.S. Nisar, M. Zakarya, A.H. Abdel-Aty, Evaluating the unsteady Casson nanofluid over a stretching sheet with solar thermal radiation: an optimal case study, Case Stud. Therm. Eng. 26 (2021), 101148.

[15] Z. Abdelmalek, A. Hussain, S. Bilal, M. Sherif, P. Thounthong, Brownian motion and thermophoretic diffusion influence on thermophysical aspects of electrically conducting viscoelastic nanofluid flow over a stretched surface, J. Mater. Res. Technol. 9 (5) (2020) 11948–11957.

[16] A.R. Hassan, S.O. Salawu, A.B. Disu, O.R. Aderele, Thermodynamic analysis of a tangent hyperbolic hydromagnetic heat generating fluid in quadratic Boussinesq approximation, J. Comput. Math. Data Sci. 4 (2022), 100058.

[17] M.D. Shamshuddin, F. Mabood, W.A. Khan, Govind R. Rajput, Exploration of thermal Peclet number, vortex viscosity and Reynolds number on two-dimensional flow of micropolar fluid through a channel due to mixed convection, Heat Tran. (2022), https://doi.org/10.1002/htj.22719.

[18] M.M. Bhatti, T. Abbas, M.M. Rashidi, M.E. Ali, Z. Yang, Entropy generation on MHD eyring–powell nanofluid through a permeable stretching surface, Entropy 18 (2016) 224.

[19] M.S. Khan, S. Mei, Shabnam, U. Fernandez-Gamiz, S. Noeiaghdam, S.A. Shah, A. Khan, Numerical analysis of unsteady hybrid nanofluid flow comprising CNTs-ferrous oxide/water with variable magnetic field, Nanomaterials 12 (2022) 180.

[20] S.O. Salawu, A.M. Obalalu, M.D. Shamshuddin, Nonlinear solar thermal radiation efficiency and energy optimization for magnetized hybrid Prandtl-Eyring nanoliquid in aircraft, Arabian J. Sci. Eng. 22 (2022), 070801.

[21] N. Kakar, A. Khalid, A.S. Al-Johani, N. Alshammari, I. Khan, Melting heat transfer of a magnetized water-based hybrid nanofluid flow past over a stretching/shrinking wedge, Case Stud. Therm. Eng. 30 (2022), 101674.

[22] G. Ravi Kiran, M.D. Shamshuddin, C.B. Krishna, K. Rajesh, Mathematical modeling of extraction of the underground fluids: application to peristaltic transportation through a vertical conduit occupied with a porous material, IOP Conf. Ser. Mater. Sci. Eng. (2020) 981.

[23] M. Khan, M.Y. Malik, T. Salahuddin, Heat generation and solar radiation effects on Carreau nanofluid over a stretching sheet with variable thickness: using coefficients improved by Cash and Carp, Results Phys. 7 (2017) 2512–2519.

[24] S.O. Salawu, R.A. Oderinu, A.D. Ohaegbue, Current density and thermodynamic analysis of energy optimization for double exothermic reaction of magneto-Oldroyd 8-constant material, J. King Saud Univ. Sci. 33 (3) (2021), 101374.

[25] B. Unyong, R. Vadivel, M. Govindaraju, R. Anbuvithya, N. Gunasekaran, Entropy analysis for ethylene glycol hybrid nanofluid flow with elastic deformation, radiation, non-uniform heat generation/absorption, and inclined Lorentz force effects, Case Stud. Therm. Eng. 30 (2022), 101639.

[26] R.P. Sharma, S.M. Ibrahim, S.R. Mishra, S. Tinker, Impact of dissipative heat and radiative heat on MHD viscous flow through a slandering stretching sheet with temperature-dependent variable viscosity, Heat Tran. (2021) 1–20.

[27] F. Mabood, K. Das, Melting heat transfer on hydromagnetic flow of a nanofluid over a stretching sheet with radiation and second-order slip, Eur. Phys. J. Plus 3 (2016) 131.

[28] Y. Chen, C.M. Chen, Numerical algorithm for solving the Stokes' first problem for a heated generalized second grade fluid with fractional derivative, Numer. Algorithm. 77 (3) (2017) 939–953.

[29] I. Khan, K.A. Abro, M.N. Mirbhar, I. Tlili, Thermal analysis in Stokes' second problem of nanofluid: applications in thermal engineering, Case Stud. Therm. Eng. 12 (2018) 271–275.

[30] E.A. Bedrikova, A.V. Latyshev, Analytical solution of the second Stokes problem with variable amplitude on behavior of gas over an oscillation surface, J. Phys. Conf. 788 (2017), 012038.

[31] N. Ishfaq, W.A. Khan, Z.H. Khan, The Stokes' second problem for nanofluids, J. King Saud Univ. Sci. 5 (2017), 05001.

[32] J.S. Duan, X. Qiu, Stokes' second problem of viscoelastic fluids with constitutive equation of distributed-order derivative, Appl. Math. Comput. 331 (2018) 130–139.

[33] C.H. Hor, C.P. Tso, G.M. Chen, Viscous dissipation in asymmetrical thermal boundaries microchannels in extended Stokes's second problem, Case Stud. Therm. Eng. 38 (2022), 102291.

[34] I.G. Currie, Fundamental Mechanics of Fluids, fourth ed., CRC Press, 2012.